Molecular Vision 2004; 10:996-1004 <http://www.molvis.org/molvis/v10/a118>
Received 17 August 2004 | Accepted 6 December 2004 | Published 27 December 2004

Advanced glycation endproduct modified basement membrane attenuates endothelin-1 induced $[Ca^{2+}]_i$ signalling and contraction in retinal microvascular pericytes

Sarah-Jane Hughes,[1] Noreen Wall,[1] C. Norman Scholfield,[2] J. Graham McGeown,[2] Tom A. Gardiner,[1] Alan W. Stitt,[1] Tim M. Curtis[1]

[1]Centre of Vision Science, Institute of Clinical Sciences, The Royal Victoria Hospital and [2]Smooth Muscle Group, Medical Biology Center, The Queen's University of Belfast, Belfast, Northern Ireland

Purpose: To assess the effects of advanced glycation endproduct (AGE) modification of vascular basement membrane (BM) on endothelin-1 (Et-1) induced intracellular $[Ca^{2+}]$ ($[Ca^{2+}]_i$) homeostasis and contraction in retinal microvascular pericytes (RMP).

Methods: RMPs were isolated from bovine retinal capillaries and propagated on AGE modified BM extract (AGE-BM) or non-modified native BM. Cytosolic Ca^{2+} was estimated using fura-2 microfluorimetry and cellular contraction determined by measurement of planimetric cell surface area. ET_A receptor mRNA and protein expression was assessed by real time RT-PCR and western blotting, respectively.

Results: Exogenous endothelin-1 (Et-1) evoked rises in $[Ca^{2+}]_i$ and contraction in RMPs were found to be mediated entirely through ET_A receptor (ET_AR) activation. Both peak and plateau phases of the Et-1 induced $[Ca^{2+}]_i$ response and contraction were impaired in RMPs propagated on AGE modified BM. ET_AR mRNA expression remained unchanged in RMPs exposed to native or AGE-BM, but protein expression for ET_AR (66 kDa) was lower in the AGE exposed cells.

Conclusions: These results suggest that substrate derived AGE crosslinks can influence RMP physiology by mechanisms which include disruption of ET_A receptor signalling. AGE modification of vascular BMs may contribute to the retinal hemodynamic abnormalities observed during diabetes.

As contractile cells attached to the wall of capillaries, pericytes are thought to be particularly important in the retina where the ratio of these cells to vascular endothelial cells is greater than in any other microvascular bed [1]. A distinctive feature of the retinal microvasculature is the absence of any pre-capillary sphincters, which in other tissues regulate capillary perfusion [2]. The absence of these sphincters suggests that local perfusion within the retina is controlled, at least in part, at the capillary level. Contraction and relaxation of retinal microvascular pericytes (RMPs) is thought to regulate the luminal diameter of retinal capillaries [3-5] and these cells are believed to play a major role in adjusting blood flow through the retinal capillary beds.

Secretion of neurotransmitters from autonomic nerve terminals is a mechanism frequently observed in many circulatory systems to control changes in vessel caliber. The retinal microcirculation, however, has a unique lack of autonomic innervation past the optic nerve head, indicating the existence of alternative regulatory mechanisms [6]. Hence, it is believed that RMP tone is regulated locally in response to endothelial and retinal derived vasomodulators acting in paracrine fashion. A number of studies have examined the vasoreactivity of RMPs in vitro. ATP, angiotensin II, and endothelin-1 (Et-1) have been identified as contracting factors [7-9] whereas nitric oxide (NO) and adenosine elicit a relaxing effect [10,11].

The most potent vasoconstrictor released by the endothelium is Et-1 and this is known to contribute to basal vascular tone in the retina [12]. Two types of endothelin receptor have been characterized in mammalian tissues, namely ET_A and ET_B receptors, and studies have demonstrated that RMPs possess both receptor subtypes [13]. The contractile effect of Et-1 is mediated entirely through ET_A receptors in retinal microvessels [14]. Receptor occupation leads to the activation of the inositol phosphate signalling pathway and Ca^{2+} release from intracellular stores which, in the presence of calmodulin and myosin light chain kinase, activates the contractile mechanism [15].

Clinical studies of retinal hemodynamic changes in diabetes indicate that increased blood flow and impaired autoregulation are features of diabetic retinopathy (DR) and may contribute to pathogenesis of this disease [16,17]. Indeed, patients who fail to demonstrate improvement of hemodynamic indices through normalization of blood glucose on follow-up, tend to show a more rapid progression of disease [18]. Within in vitro systems, RMPs cultured under high ambient glucose exhibit reduced contractile responses following stimulation with Et-1 [19]. Furthermore, in diabetes the retinal blood vessels become resistant to the actions of Et-1 [20,21], and this, in combination with the enhanced production of vasodilators [22,23], could explain why an increase in blood flow is ob-

Correspondence to: Dr. Tim Curtis, Centre of Vision Science, The Queen's University of Belfast, Institute of Clinical Sciences, Grovenor Road, The Royal Victoria Hospital, Belfast, Northern Ireland, BT12 6BA; Phone: +44 028 90635027; FAX: +44 028 90632699; email: t.curtis@qub.ac.uk

served. Several independent investigators have related vasoconstrictor insensitivity to increased activation of protein kinase C, an enzyme recognised to alter Ca^{2+} homeostasis in retinal vessels [24,25]. However, recent studies have suggested that other glucose mediated pathogenic mechanisms, including formation of advanced glycation endproducts (AGEs), may also impair agonist induced intracellular Ca^{2+} signalling [26-28]. AGEs have been shown to accumulate in the intra- and extracellular domains of retinal blood vessels [29] and this may induce a range of pathophysiological responses in retinal pericytes [30].

Motivated by these considerations, the current study was designed to examine whether AGE modification of the vascular basement membrane alters Et-1 induced Ca^{2+} signalling and contraction (change in 2-dimensional surface area) in retinal pericytes. Efforts have also been made to delineate the molecular mechanisms responsible for the changes observed.

METHODS

Isolation of retinal microvascular pericyte (RMP) cells: Bovine eyes were obtained from a local abattoir and RMPs were isolated by selective sieving and digestion as previously described [31]. The cells were propagated on T25 Falcon flasks (Fisher Scientific, Loughborough, UK) in Dulbecco's modified Eagle's medium (DMEM; Invitrogen, Paisley, UK) containing 5 mM glucose and 20% fetal calf serum (FCS; Invitrogen). Preliminary intracellular $[Ca^{2+}]$ ($[Ca^{2+}]_i$) experiments (see below) showed that bovine retinal pericytes become less responsive to Et-1 (10 nM) at passages 3 and above, and consequently cells beyond passage 2 were not used.

Preparation of AGE modified basement membrane (BM): AGE modified BM was prepared as described [32]. In brief, Matrigel (BD Biosciences, Oxford, UK) was diluted 1:10 with DMEM containing 50 mg/ml Normocin (InvivoGen, San Diego, CA). A thin layer of Matrigel was applied to the surface of the tissue culture vessel or glass coverslips depending on the experimental protocol and allowed to polymerize for 1 h at 37 °C. AGE modification of Matrigel was achieved through exposure to 50 mM glycoaldehyde in PBS (145 mM NaCl, 30 mM $Na_2H_2PO_4$, and 95 mM Na_2HPO_4, pH 7.3) for 4 h at 37 °C. The glycation reaction was then terminated by incubation with glycine ethyl ester (1 M in PBS) for 1 h at 37 °C. The AGE modified matrigel was rinsed thrice with PBS and further incubated in PBS overnight to completely remove any residual glycoaldehyde and glycine ethyl ester. Control matrices (native BM) were treated in a similar fashion without the addition of glycoaldehyde. We have previously established that 10-100 mM glycoaldehyde modification of Matrigel for 4 h results in the formation of distinct AGE profiles, with approximately 10 fold higher levels of N^e-(carboxymethyl)lysine (CML) and negligible formation of N^e-(carboxyethyl)lysine (CEL) when compared to extracellular matrix from diabetic animal models [30,33].

$[Ca^{2+}]_i$ measurements: $[Ca^{2+}]_i$ was estimated fluorometrically in cultured RMPs loaded with the intracellular Ca^{2+} probe fura-2 AM (Biotium, Hayward, CA). For these experiments, cells were passed onto glass coverslips coated with native BM or AGE modified BM. After 12 h the RMPs were loaded in the dark for 1 h at 37 °C with 5 μM fura-2. The coverslips bearing the adherent cells were then placed in a recording bath mounted on an inverted microscope (Eclipse TE300 from Nikon, Kingston Upon Thames, UK) with a final magnification of 600x. Hanks solution (140 mM NaCl, 5 mM KCl, 5 mM D(+) glucose, 1.3 mM $MgCl_2$, 2 mM $CaCl_2$, 10 mM HEPES (free acid), pH 7.3) was allowed to flow into one end of the bath and was withdrawn from the other at 2 ml/min. The solution passed through a heat exchanger to ensure that the temperature in the recording bath was maintained at 37 °C. The system for the delivery of solutions, including those containing drugs, consisted of a manifold (volume 3 μl) into which seven separate reservoirs fed. Its outlet was positioned about 500 μm away from the cell of interest. The flow into the bath and over the cells was streamlined and the delay time for new solution to reach the cell of interest was 1 s as measured by switching to a dye solution [14]. Et-1 and BQ123 were from Tocris (Bristol, UK) and American Peptide Corporation (Sunnyvale, CA), respectively.

Cells of interest, defined as those that had spread substantially on their underlying substratum, were illuminated by 340/380 nm light from a dual monochromator (5 nm bandwidth) and a light chopper (Cairn Research Ltd., Faversham, UK). Emitted fluorescence was measured from the side port of the microscope via an adjustable rectangular window, a filter (510 nm) and a photon counting photomultiplier tube (PMT) in the light path. Fluorescence equipment was controlled by Acquisition Engine (Cairn) software (version 1.1.5) which also performed the storage and analysis of the fluorescence data.

Upon completion of an experimental protocol, the fura-2 in the cell was quenched with Ca^{2+}-free Hanks solution containing 5 mM $MnCl_2$. The delivery of this solution continued until fluorescence counts had declined to a constant level. The remaining unquenched fluorescence was used as a background to subtract from the fluorescence signal. The ratio maximums (R_{max}, 4.2; n=10) and minimums (R_{min}, 0.4; n=12) of the 340/380 counts were obtained using ionomycin (1 μM; Sigma, Poole, UK) containing 100 mM Ca^{2+} or Ca^{2+} free/1 mM EGTA Hanks solution, respectively. For the in-cell dissociation constant for fura-2 (K_D), which was measured as 94 nM, RMPs were exposed to a range of solutions containing increasing Ca^{2+} concentrations and 1 μM ionomycin. $[Ca^{2+}]_i$ was estimated from the 380/340 fluorescence ratio using the relationship of Grynkiewicz et al. [34].

Cell contraction: Contraction of RMPs was determined by measurement of planimetric cell surface area, using image analysis (Nikon Lucia, Nikon, Kingston Upon Thames, UK), from a library of imported images acquired using a frame grabber (Data Translation, Marlboro, MA) coupled with screen recording software (Hypercam, Hyperionics, Murrayfield, PA; Version 2.10.02). Cells were allowed to adhere to native BM or AGE-BM coated coverslips for 12 h as described above and superfused with Hanks solution at 37 °C, on an inverted microscope with a final magnification of 400x. RMPs were pre-relaxed with forskolin (10 mM; Tocris, Avonmouth, UK), an elevator of intracellular cyclic adenosine monophosphate,

for 10 min before stimulation with Et-1. In addition to providing a common baseline, the pre-administration of forskolin seemed to sensitize the contractile machinery to Et-1 since in its absence the cells displayed only partial contraction. During image analysis, RMP edges were identified with automated threshold detection, and cell surface area changes were measured by means of a hand held cursor which was used to outline the perimeter of the cell.

ET_A receptor expression: RMPs used for these studies were cultured for 12 h on T25 flasks treated as previously outlined. RMP total RNA was extracted using TRI REAGENT™ (Sigma). The quantity of RNA in each experimental group was determined spectrophotometrically (U1100 model, Hitachi Europe Ltd., Maidenhead, UK) and the purity and quality of each RNA sample was estimated by visualization of clear 18S and 28S ribosomal RNA bands after electrophoresing 2 μg of each sample on a 1% agarose gel.

Reverse transcription was performed with Superscript II reverse transcriptase (Invitrogen, Paisley, UK), primed with random hexanucleotides (Roche, Lewes, UK). Real-time RT-PCR was conducted for quantitative analysis of mRNA expression using sequence specific primers for bovine ET_A receptor (Forward: 5'-AGT CGT GTT CAG GGA ATT GG-3' and Reverse: 5'-AAG GTA CCA TGA CAA AGC CG-3', yielding a 115 bp fragment). Primers to amplify the housekeeping gene, acidic ribosomal phosphoprotein (ARP: Forward 5'-CGA CCT GGA AGT CCA ACT AC-3' and Reverse: 5'-ATC TGC TGC ATC TGC TTG-3', yielding a 109 bp fragment), and 28S rRNA (Forward: 5'-TTG AAA ATC CGG GGG AGA G-3' and Reverse: 5'-ACA TTG TTC CAA CAT GCC AG-3' yielding a 100 bp fragment) were also designed. Primers were designed from mouse, rat, and human conserved regions.

Real-time PCR was performed using a LightCycler rapid thermal cycler system (Roche, Welwyn Garden City, UK) according to protocols outlined by Simpson et al. [35]. The PCR reaction was performed in glass capillary reaction vessels in a 20 μl volume with 0.5 mM primers. Reaction buffer, 2.5 mM $MgCl_2$, dNTPs, Hotstart Taq DNA polymerase and SYBR Green I were included in the QuantitTect LightCycler-SYBR

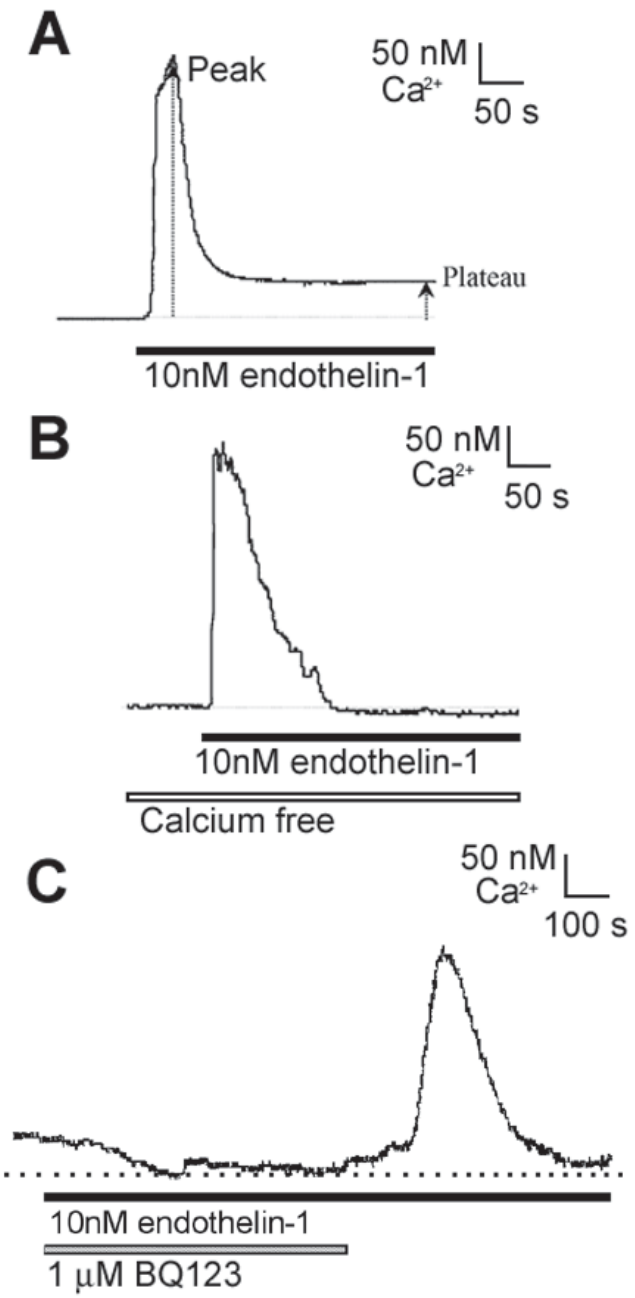

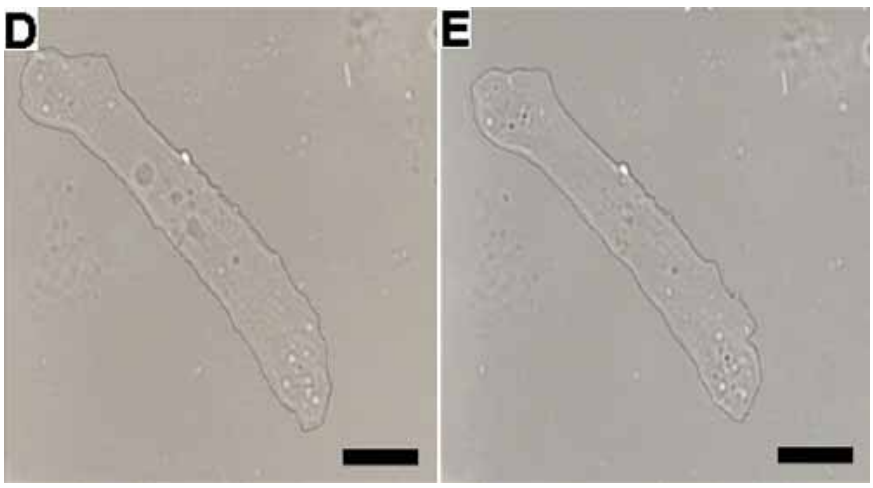

Figure 1. Et-1 activates a BQ123 sensitive calcium transient and contractile response in RMPs cultured on native BM. **A**: Typical record among 10 trials showing that 10 nM Et-1 evokes a biphasic Ca^{2+} response in RMPs comprising a peak and plateau phase. **B**: Application of Et-1 in a Ca^{2+}-free Hanks solution causes elimination of the plateau phase (n=6). **C**: The reversible ET_A receptor antagonist BQ123 (1 μM), prevents the Et-1 $[Ca^{2+}]_i$ response, while washing out in normal Hanks solution is able to restore the effect (n=6). **D**: Light micrograph of a pericyte before Et-1 stimulation. **E**: Light micrograph of a pericyte 10 min after Et-1 stimulation (in the absence of forskolin). Scale bars for **D** and **E** represent 20 μm.

Green PCR Master Mix (Qiagen, Crawley, UK). All reactions were performed for 40 repeats of the following cycle: 15 s at 94 °C, 15 s at 50 °C, and 20 s at 72 °C. The specificity of the amplification reactions was confirmed by melting curve analysis and subsequently by agarose gel electrophoresis [35]. For each gene, PCR amplifications were performed in triplicate on three independent RT reactions.

SDS-PAGE and western immunoblotting: Whole cell protein samples of RMP that were grown on AGE-BM or native-BM controls for 12 h were prepared by scraping the cells off the flasks in an extraction buffer solution of PBS containing protease inhibitors (Complete™ Mini, Boehringer Mannheim, Mannheim, Germany). The samples were solubilized and the protein concentration was determined using the BCA protein kit (Pierce, Rockford, IL). SDS-PAGE was conducted according to standard protocols [36] with protein samples (30 μg) diluted in Laemmli lysis buffer (Bio-Rad, Richmond, CA) containing 5% (V/V) β-mercaptoethanol. Equal amounts of each protein sample were separated on denaturing 4-20% SDS gels (Bio-Rad) and transferred onto nitrocellulose membrane (Bio-Rad). After blocking, the membrane was incubated overnight with a polyclonal antibody to the ET_A receptor (anitibody diluted to 0.9 μg/ml; product number AER-001 from Alomone Laboratories, Jerusalem, Israel). After washing, the membrane was then incubated in a goat anti-rabbit secondary antibody with a horseradish peroxidase conjugate (Dako Ltd., Ely, UK) for 2 h. Labeled protein was detected using enhanced chemiluminesence (Amersham, Little Chalfont, UK) exposed to Hyperfilm X-ray film (Amersham) in a dark room. To confirm equal protein loading, the blot was re-probed with a primary monoclonal antibody, diluted to 0.1 μg/ml, against HSC-70 (constitutive heat shock protein, 70 kDa, Stressgen Biotechnologies, Victoria, Canada) and using an appropriate secondary antibody (anti-rat HRP). To obtain quantitative data for protein expression, the developed ET_A receptor immunoblot was placed in the GeneGenius bio-imaging system (Synaptics Ltd., Cambridge, UK), and the density of each band (relative light units) was measured individually using Syngene software (Synaptics Ltd.; version 3.1).

Statistical analysis: Data are presented as means and standard error of the mean (SEM). Unpaired comparisons were made using the Student's t-test and data were considered significant at 95% ($p<0.05$). Percentage data were arcsine transformed to normalize the distribution prior to performing statistical analyses. Each experiment was conducted at least three times, and the exact number is given in the figure legends.

RESULTS

Et-1 induced calcium transients and contraction: When stimulated with Et-1 (10 nM), RMPs exhibited a biphasic $[Ca^{2+}]_i$ response (Figure 1A) characterized by an initial transient peak in $[Ca^{2+}]_i$ followed by a sustained plateau phase during which the $[Ca^{2+}]_i$ remained elevated above basal levels. RMPs also exhibited a discernible reduction in planimetric cell surface area, in response to Et-1 (Figure 1D). RMPs exposed to Et-1 in a Ca^{2+}-free Hanks solution, showed a monophasic response characterized by a rapid transient increase in $[Ca^{2+}]_i$ which subsequently fell back down to resting levels (Figure 1B). In these experiments, abolition of the characteristic plateau component suggests that the plateau phase of the Et-1 induced $[Ca^{2+}]_i$ response probably results from Ca^{2+} influx across the plasma membrane. BQ123 (1 μM), a reversible ET_A receptor antagonist [37-39], prevented the Et-1 mediated rises in $[Ca^{2+}]_i$, an effect that was reversed following washout in Hanks solution (Figure 1C). These observations demonstrate that the $[Ca^{2+}]_i$ response evoked by Et-1 was mediated entirely through ET_A receptors.

When stimulated with Et-1, RMPs grown on AGE-BM demonstrated an attenuation in both peak and plateau increases

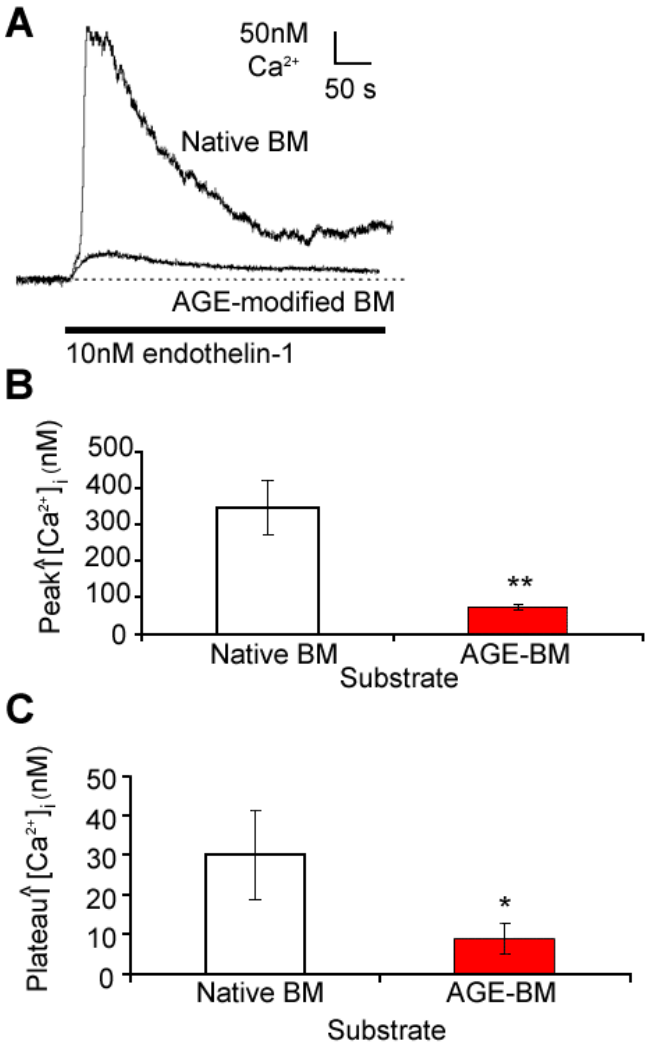

Figure 2. Et-1 induced calcium transients in RMPs cultured on native and AGE-BM. **A**: Representative traces showing that both peak and plateau increases in $[Ca^{2+}]_i$ with Et-1 are severely impaired in RMPs cultured on AGE-BM. **B**: Mean data demonstrating that peak increases in $[Ca^{2+}]_i$ with Et-1 are depressed for native BM (n=11) compared to AGE-BM (n=15). Double asterisk (**) indicates $p<0.01$. **C**: Mean data demonstrating that plateau increases in $[Ca^{2+}]_i$ with Et-1 are depressed for native BM (n=11) compared to AGE-BM (n=15). Asterisk (*) indicates $p<0.05$.

in $[Ca^{2+}]_i$, when compared with cells grown on native BM (Figure 2). RMPs cultured on AGE-BM also showed a decreased ability to contract in response to Et-1 (Figure 3).

ET_A receptor mRNA and protein levels: Having established that RMPs grown on an AGE-BM showed blunted $[Ca^{2+}]_i$ and contractile responses to Et-1, the next series of experiments were designed to unravel the molecular mechanisms involved. We considered that perhaps ET_A receptor numbers had been reduced on cells exposed to AGE-BM. To investigate this possibility we implemented a two pronged approach, examining both ET_A receptor mRNA expression and protein levels.

Real-time RT-PCR was conducted to compare ET_A mRNA expression when RMPs were propagated on AGE-BM or native-BM. No differences in ET_A mRNA expression were observed between the two treatment groups (Figure 4A).

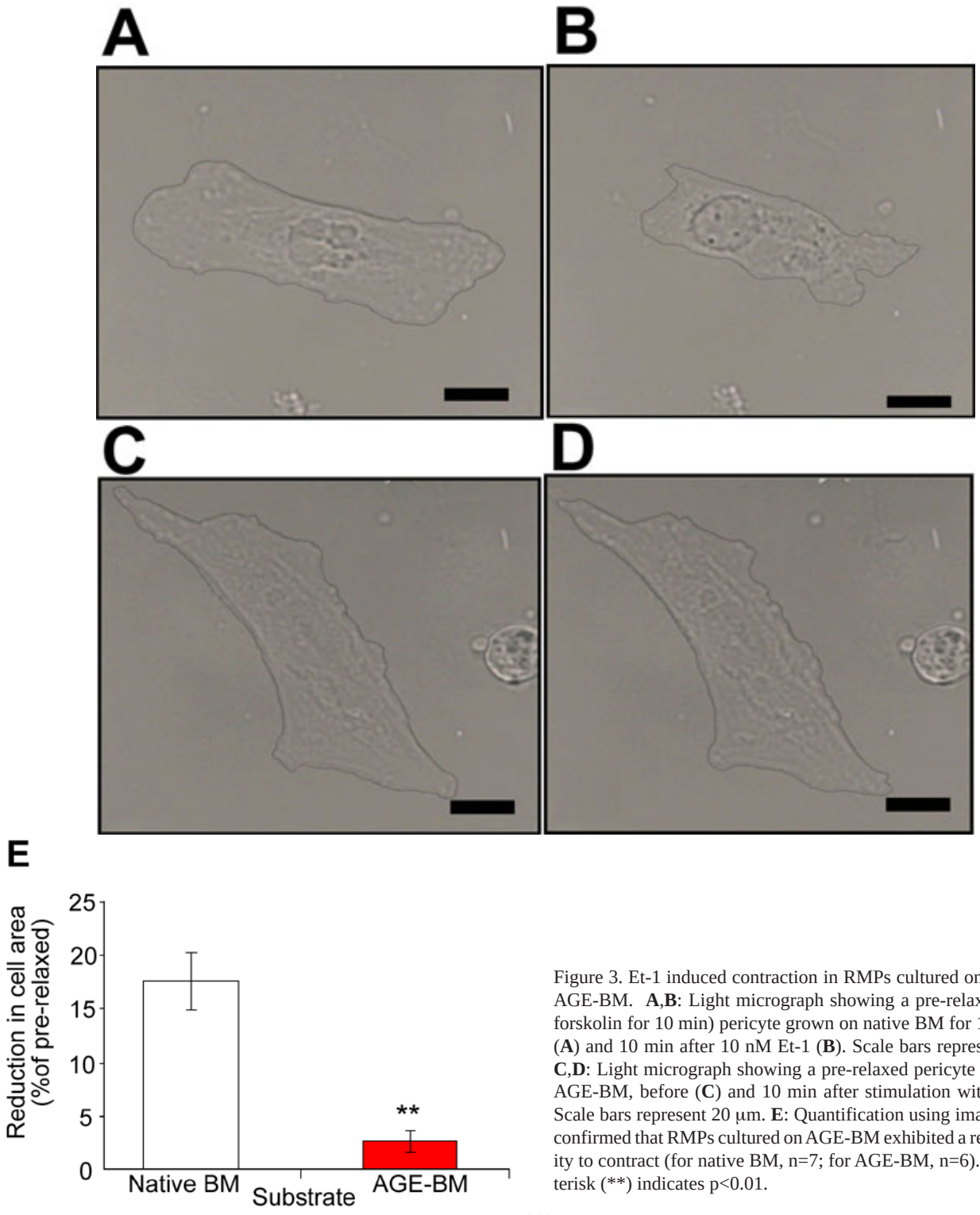

Figure 3. Et-1 induced contraction in RMPs cultured on native and AGE-BM. **A**,**B**: Light micrograph showing a pre-relaxed (10 μM forskolin for 10 min) pericyte grown on native BM for 12 h, before (**A**) and 10 min after 10 nM Et-1 (**B**). Scale bars represent 20 μm. **C**,**D**: Light micrograph showing a pre-relaxed pericyte cultured on AGE-BM, before (**C**) and 10 min after stimulation with Et-1 (**D**). Scale bars represent 20 μm. **E**: Quantification using image analysis confirmed that RMPs cultured on AGE-BM exhibited a reduced ability to contract (for native BM, n=7; for AGE-BM, n=6). Double asterisk (**) indicates $p<0.01$.

Western blotting of whole cell RMP fractions indicated the migration of two anti-ET_A immunoreactive protein species, with apparent molecular weights of 66 kDa and 38 kDa (Figure 4B). The low molecular weight band observed corresponded to a proteolytic fragment of the high molecular weight protein, which still possesses the ligand binding properties of the receptor [40]. Quantification by densitometry revealed that RMPs cultured on AGE-BM showed a decline in ET_A receptor (66 kDa) levels in comparison to controls (Figure 4C). In contrast, levels of the proteolytic component (38 kDa) of the ET_A receptor remained unchanged (Figure 4D).

DISCUSSION

In RMPs, activation of ET_A receptors by Et-1 stimulated both Ca^{2+} mobilization from intracellular stores and Ca^{2+} influx from the extracellular medium. Although the definitive Ca^{2+} handling mechanisms have yet to be elucidated in RMPs, considerable efforts have been made to delineate these in retinal microvascular smooth muscle (MVSM) cells and it is now recognised that Et-1 induced Ca^{2+} release from the endoplasmic reticulum results from activation of the IP_3 pathway [14]. In RMPs the Ca^{2+} influx phase with Et-1 can be inhibited by diltiazem and consequently has been attributed to the activation of voltage dependent L-type Ca^{2+} channels [41]. However, recent work has suggested that such antagonists are also capable of blocking voltage independent Ca^{2+} influx pathways [42]. Moreover, in choroidal MVSM cells Et-1 reduces rather than accentuates the L-type Ca^{2+} current [43]. Thus it seems most likely that the plateau phase of the Et-1 induced $[Ca^{2+}]_i$ response in RMPs results from Ca^{2+} influx through store and

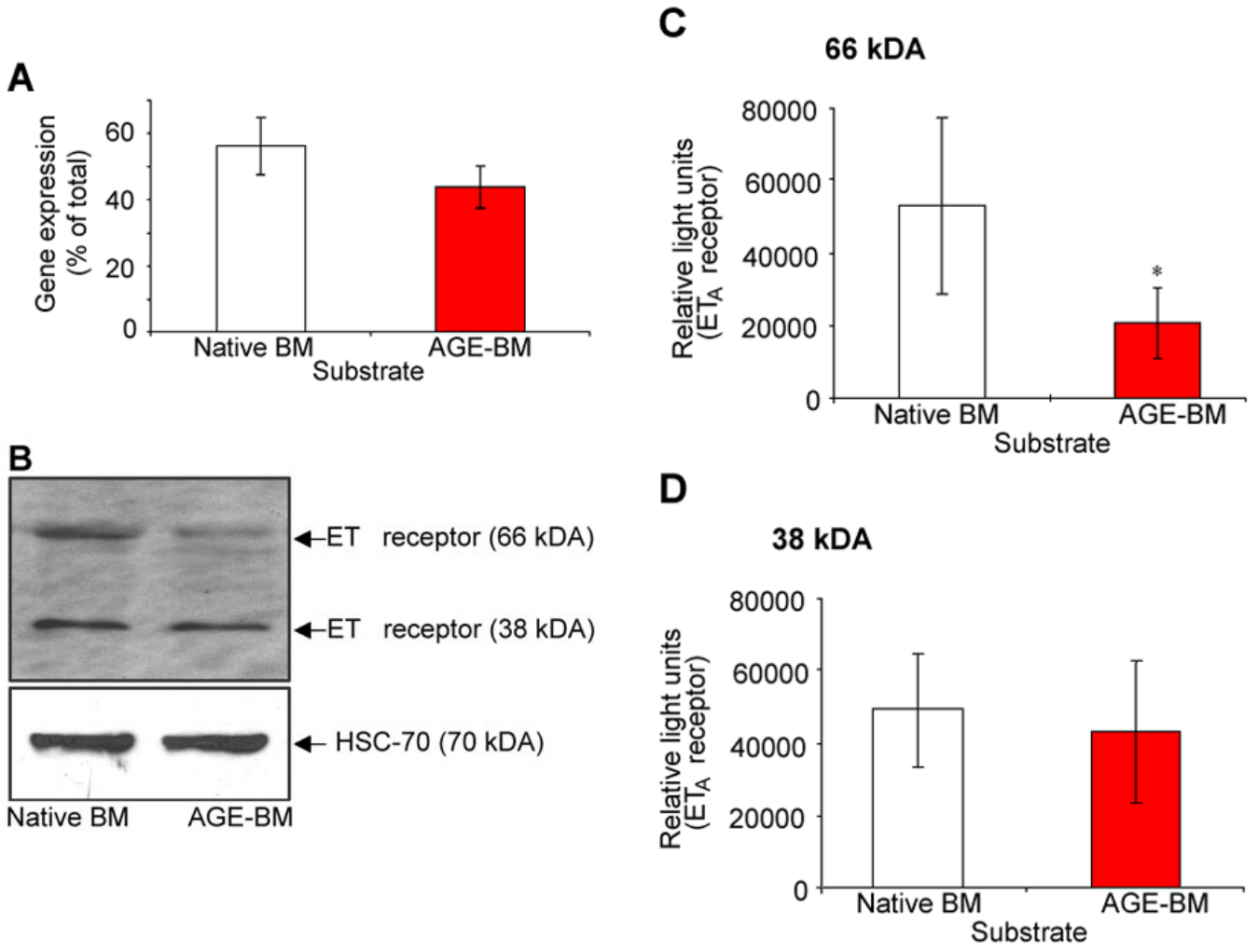

Figure 4. ET_A receptor mRNA and protein expression in RMPs cultured on native and AGE-BM. **A**: RT-PCR indicated that there was a no change in ET_A receptor mRNA expression following exposure of RMPs to AGE-BM. Data were normalized to rRNA and acidic ribosomal phosphoprotein, whose expression was unchanged on AGE-BM ($p<0.05$). Each column represents the mean of 3 independent experiments. Variability in absolute levels of gene expression (arbitary values) among replicates was eliminated by dividing the ET_A receptor expression for the individual treatments by the sum total of gene expression under both conditions and this value then expressed as a percentage. **B**: Western blot showing the expression of two ET_A receptor species following exposure of RMPs to AGE-BM. The western blot was re-probed with an antibody to HSC-70 to confirm equal protein loading. **C**,**D**: Densitometric analysis revealed that there was a reduction in the 66 kDa ET_A receptor species and no change in the 38 kDa ET_A receptor proteolytic fragment with AGE modified BM. Each column represents the mean of 6 individual experiments. Asterisk (*) indicates $p<0.05$.

receptor operated Ca^{2+} channels.

Formation of AGEs on intracellular proteins [44-46] and the extracellular matrix (ECM) [47,48] is thought to play an important role in the pathogenesis of diabetic complications and these adducts are known to accumulate in the microvessels and retinal neuroglia of diabetic retinas [29,49,50]. In diabetic rats, immunoreactive AGEs are detected in retinal vascular BMs and accumulate as a function of diabetes duration [29]. The pathogenic consequences of AGE modification of BMs have not been well studied; however, it is recognized that cell dysfunction could arise through alteration of cell-ECM interactions [51] or via AGE receptor mediated generation of reactive oxygen species [52,53].

In the current study, we provide evidence that AGE modification of a vascular BM inhibits Et-1 mediated Ca^{2+} signalling and contractile responses in RMPs. Aberrations in Ca^{2+} mobilization appeared nonspecific since both peak and plateau phases of the responses were affected to a similar degree. These data concur with those of Bishara et al. [27] who demonstrated that agonist evoked intracellular Ca^{2+} release and store operated Ca^{2+} influx are impaired in endothelial cells adhering to an AGE-BM. They are also consistent with our previous observations in retinal microvessels from diabetic animals (3 month disease duration), where Et-1 induced Ca^{2+} mobilization [21] is severely depressed. This adds weight to the hypothesis that AGE modification of vascular BMs may play a major role in mediating the retinal vasoregulatory abnormalities seen in diabetes. Moreover, it is probable that a number of other Ca^{2+} regulated cellular events, such as BM component synthesis [54] and degradation [55] to cell death [30] may be affected by diabetes mediated crosslinking of cell substrates.

Since the Et-1 induced Ca^{2+} transients were attenuated in a generalized fashion, we considered ET_A receptor downregulation to be the most likely explanation for this. Our data shows that ET_A receptor gene transcription is unaffected in RMPs by AGE modification of BM. However, we have presented clear evidence that ET_A receptor protein expression (66 kDa) is reduced. The findings of the present study suggest that AGE modification of vascular BM may lead to reduction in mRNA translation within attachment dependent cells such as RMPs and/or impact on post-translational processes, such as enhancing the activity of the ubiquitin-proteosome pathway, which is known to regulate the expression of G-protein coupled receptors like the ET_A receptor [56]. Indeed, the activity of the ubiquitin-proteosome proteolytic pathway has been shown to be upregulated in the diabetic state [57,58] and by exposure to AGEs [59].

In summary, these results demonstrate that AGE modified BM can impact on Et-1 induced $[Ca^{2+}]_i$ homeostasis and contractility in RMPs through a mechanism which appears to involve downregulation of ET_A receptor protein expression. Abnormal $[Ca^{2+}]_i$ homeostasis and contractility, elicited by advanced glycation of the extracellular matrix, may contribute to the retinal hemodynamic changes in diabetes and ultimately to the demise of retinal microvascular mural cells during DR.

ACKNOWLEDGEMENTS

We thank the Royal National Institute for the Blind, Diabetes UK, The Juvenile Diabetes Research Foundation, and the R&D Office, Northern Ireland for financial support. We are grateful to Dr. David Simpson for assistance with PCR analysis.

REFERENCES

1. Balabanov R, Dore-Duffy P. Role of the CNS microvascular pericyte in the blood-brain barrier. J Neurosci Res 1998; 53:637-44.
2. Pannarale L, Onori P, Ripani M, Gaudio E. Precapillary patterns and perivascular cells in the retinal microvasculature. A scanning electron microscope study. J Anat 1996; 188:693-703.
3. Schonfelder U, Hofer A, Paul M, Funk RH. In situ observation of living pericytes in rat retinal capillaries. Microvasc Res 1998; 56:22-9.
4. Sakagami K, Kodama T, Puro DG. PDGF-induced coupling of function with metabolism in microvascular pericytes of the retina. Invest Ophthalmol Vis Sci 2001; 42:1939-44.
5. Wu DM, Kawamura H, Sakagami K, Kobayashi M, Puro DG. Cholinergic regulation of pericyte-containing retinal microvessels. Am J Physiol Heart Circ Physiol 2003; 284:H2083-90.
6. Ye XD, Laties AM, Stone RA. Peptidergic innervation of the retinal vasculature and optic nerve head. Invest Ophthalmol Vis Sci 1990; 31:1731-7.
7. Das A, Frank RN, Weber ML, Kennedy A, Reidy CA, Mancini MA. ATP causes retinal pericytes to contract in vitro. Exp Eye Res 1988; 46:349-62.
8. Matsugi T, Chen Q, Anderson DR. Contractile responses of cultured bovine retinal pericytes to angiotensin II. Arch Ophthalmol 1997; 115:1281-5.
9. Chakravarthy U, Gardiner TA, Anderson P, Archer DB, Trimble ER. The effect of endothelin 1 on the retinal microvascular pericyte. Microvasc Res 1992; 43:241-54.
10. Haefliger IO, Zschauer A, Anderson DR. Relaxation of retinal pericyte contractile tone through the nitric oxide-cyclic guanosine monophosphate pathway. Invest Ophthalmol Vis Sci 1994; 35:991-7.
11. Matsugi T, Chen Q, Anderson DR. Adenosine-induced relaxation of cultured bovine retinal pericytes. Invest Ophthalmol Vis Sci 1997; 38:2695-701.
12. Takagi C, Bursell SE, Lin YW, Takagi H, Duh E, Jiang Z, Clermont AC, King GL. Regulation of retinal hemodynamics in diabetic rats by increased expression and action of endothelin-1. Invest Ophthalmol Vis Sci 1996; 37:2504-18.
13. McDonald DM, Bailie JR, Archer DB, Chakravarthy U. Characterization of endothelin A (ETA) and endothelin B (ETB) receptors in cultured bovine retinal pericytes. Invest Ophthalmol Vis Sci 1995; 36:1088-94.
14. Scholfield CN, Curtis TM. Heterogeneity in cytosolic calcium regulation among different microvascular smooth muscle cells of the rat retina. Microvasc Res 2000; 59:233-42.
15. Schiffrin EL, Touyz RM. Vascular biology of endothelin. J Cardiovasc Pharmacol 1998; 32 Suppl 3:S2-13.
16. Kohner EM, Hamilton AM, Saunders SJ, Sutcliffe BA, Bulpitt CJ. The retinal blood flow in diabetes. Diabetologia 1975; 11:27-33.
17. Schmetterer L, Wolzt M. Ocular blood flow and associated functional deviations in diabetic retinopathy. Diabetologia 1999; 42:387-405.

18. Grunwald JE, Riva CE, Baine J, Brucker AJ. Total retinal volumetric blood flow rate in diabetic patients with poor glycemic control. Invest Ophthalmol Vis Sci 1992; 33:356-63.
19. Chakravarthy U, McGinty A, McKillop J, Anderson P, Archer DB, Trimble ER. Altered endothelin-1 induced contraction and second messenger generation in bovine retinal microvascular pericytes cultured in high glucose medium. Diabetologia 1994; 37:36-42.
20. Bursell SE, Clermont AC, Oren B, King GL. The in vivo effect of endothelins on retinal circulation in nondiabetic and diabetic rats. Invest Ophthalmol Vis Sci 1995; 36:596-607.
21. Curtis TM, Scholfield CN. The role of lipids and protein kinase Cs in the pathogenesis of diabetic retinopathy. Diabetes Metab Res Rev 2004; 20:28-43.
22. Abu El-Asrar AM, Desmet S, Meersschaert A, Dralands L, Missotten L, Geboes K. Expression of the inducible isoform of nitric oxide synthase in the retinas of human subjects with diabetes mellitus. Am J Ophthalmol 2001; 132:551-6.
23. Johnson EI, Dunlop ME, Larkins RG. Increased vasodilatory prostaglandin production in the diabetic rat retinal vasculature. Curr Eye Res 1999; 18:79-82.
24. Ishii H, Jirousek MR, Koya D, Takagi C, Xia P, Clermont A, Bursell SE, Kern TS, Ballas LM, Heath WF, Stramm LE, Feener EP, King GL. Amelioration of vascular dysfunctions in diabetic rats by an oral PKC beta inhibitor. Science 1996; 272:728-31.
25. Curtis TM, Major EH, Trimble ER, Scholfield CN. Diabetes-induced activation of protein kinase C inhibits store-operated Ca2+ uptake in rat retinal microvascular smooth muscle. Diabetologia 2003; 46:1252-9.
26. Mene P, Pascale C, Teti A, Bernardini S, Cinotti GA, Pugliese F. Effects of advanced glycation end products on cytosolic Ca2+ signaling of cultured human mesangial cells. J Am Soc Nephrol 1999; 10:1478-86.
27. Bishara NB, Dunlop ME, Murphy TV, Darby IA, Sharmini Rajanayagam MA, Hill MA. Matrix protein glycation impairs agonist-induced intracellular Ca2+ signaling in endothelial cells. J Cell Physiol 2002; 193:80-92.
28. Petrova R, Yamamoto Y, Muraki K, Yonekura H, Sakurai S, Watanabe T, Li H, Takeuchi M, Makita Z, Kato I, Takasawa S, Okamoto H, Imaizumi Y, Yamamoto H. Advanced glycation endproduct-induced calcium handling impairment in mouse cardiac myocytes. J Mol Cell Cardiol 2002; 34:1425-31.
29. Stitt AW, Li YM, Gardiner TA, Bucala R, Archer DB, Vlassara H. Advanced glycation end products (AGEs) co-localize with AGE receptors in the retinal vasculature of diabetic and of AGE-infused rats. Am J Pathol 1997; 150:523-31.
30. Stitt AW, Hughes SJ, Canning P, Lynch O, Cox O, Frizzell N, Thorpe SR, Cotter TG, Curtis TM, Gardiner TA. Substrates modified by advanced glycation end-products cause dysfunction and death in retinal pericytes by reducing survival signals mediated by platelet-derived growth factor. Diabetologia 2004; 47:1735-1746.
31. Chakravarthy U, Stitt AW, McNally J, Bailie JR, Hoey EM, Duprex P. Nitric oxide synthase activity and expression in retinal capillary endothelial cells and pericytes. Curr Eye Res 1995; 14:285-94.
32. Kuzuya M, Satake S, Miura H, Hayashi T, Iguchi A. Inhibition of endothelial cell differentiation on a glycosylated reconstituted basement membrane complex. Exp Cell Res 1996; 226:336-45.
33. Degenhardt TP, Alderson NL, Arrington DD, Beattie RJ, Basgen JM, Steffes MW, Thorpe SR, Baynes JW. Pyridoxamine inhibits early renal disease and dyslipidemia in the streptozotocin-diabetic rat. Kidney Int 2002; 61:939-50.
34. Grynkiewicz G, Poenie M, Tsien RY. A new generation of Ca2+ indicators with greatly improved fluorescence properties. J Biol Chem 1985; 260:3440-50.
35. Simpson DA, Feeney S, Boyle C, Stitt AW. Retinal VEGF mRNA measured by SYBR green I fluorescence: A versatile approach to quantitative PCR. Mol Vis 2000; 6:178-83 .
36. Laemmli UK. Cleavage of structural proteins during the assembly of the head of bacteriophage T4. Nature 1970; 227:680-5.
37. Ihara M, Ishikawa K, Fukuroda T, Saeki T, Funabashi K, Fukami T, Suda H, Yano M. In vitro biological profile of a highly potent novel endothelin (ET) antagonist BQ-123 selective for the ETA receptor. J Cardiovasc Pharmacol 1992; 20 Suppl 12:S11-4.
38. Ishikawa K, Fukami T, Nagase T, Fujita K, Hayama T, Niiyama K, Mase T, Ihara M, Yano M. Cyclic pentapeptide endothelin antagonists with high ETA selectivity. Potency- and solubility-enhancing modifications. J Med Chem 1992; 35:2139-42.
39. Wu-Wong JR, Chiou WJ, Dixon DB, Opgenorth TJ. Dissociation characteristics of endothelin ETA receptor agonists and antagonists. J Cardiovasc Pharmacol 1995; 26 Suppl 3:S380-4.
40. Kozuka M, Ito T, Hirose S, Lodhi KM, Hagiwara H. Purification and characterization of bovine lung endothelin receptor. J Biol Chem 1991; 266:16892-6.
41. McGinty A, Scholfield CN, Liu WH, Anderson P, Hoey DE, Trimble ER. Effect of glucose on endothelin-1-induced calcium transients in cultured bovine retinal pericytes. J Biol Chem 1999; 274:25250-3.
42. Curtis TM, Scholfield CN. Nifedipine blocks Ca2+ store refilling through a pathway not involving L-type Ca2+ channels in rabbit arteriolar smooth muscle. J Physiol 2001; 532:609-23.
43. Curtis TM, Scholfield CN. Evidence for two endothelin Et(A) receptor subtypes in rabbit arteriolar smooth muscle. Br J Pharmacol 2001; 134:1787-95.
44. Padival AK, Crabb JW, Nagaraj RH. Methylglyoxal modifies heat shock protein 27 in glomerular mesangial cells. FEBS Lett 2003; 551:113-8.
45. Bidasee KR, Nallani K, Yu Y, Cocklin RR, Zhang Y, Wang M, Dincer UD, Besch HR Jr. Chronic diabetes increases advanced glycation end products on cardiac ryanodine receptors/calcium-release channels. Diabetes 2003; 52:1825-36.
46. Bidasee KR, Zhang Y, Shao CH, Wang M, Patel KP, Dincer UD, Besch HR Jr. Diabetes increases formation of advanced glycation end products on Sarco(endo)plasmic reticulum Ca2+-ATPase. Diabetes 2004; 53:463-73.
47. Charonis AS, Reger LA, Dege JE, Kouzi-Koliakos K, Furcht LT, Wohlhueter RM, Tsilibary EC. Laminin alterations after in vitro nonenzymatic glycosylation. Diabetes 1990; 39:807-14.
48. Degenhardt TP, Thorpe SR, Baynes JW. Chemical modification of proteins by methylglyoxal. Cell Mol Biol (Noisy-le-grand) 1998; 44:1139-45.
49. Stitt AW, Jenkins AJ, Cooper ME. Advanced glycation end products and diabetic complications. Expert Opin Investig Drugs 2002; 11:1205-23.
50. Hammes HP, Alt A, Niwa T, Clausen JT, Bretzel RG, Brownlee M, Schleicher ED. Differential accumulation of advanced glycation end products in the course of diabetic retinopathy. Diabetologia 1999; 42:728-36.
51. Paul RG, Bailey AJ. The effect of advanced glycation end-product formation upon cell-matrix interactions. Int J Biochem Cell Biol 1999; 31:653-60.
52. Yamagishi S, Inagaki Y, Amano S, Okamoto T, Takeuchi M, Makita Z. Pigment epithelium-derived factor protects cultured retinal pericytes from advanced glycation end product-induced injury through its antioxidative properties. Biochem Biophys

Res Commun 2002; 296:877-82.
53. Kaji Y, Amano S, Usui T, Oshika T, Yamashiro K, Ishida S, Suzuki K, Tanaka S, Adamis AP, Nagai R, Horiuchi S. Expression and function of receptors for advanced glycation end products in bovine corneal endothelial cells. Invest Ophthalmol Vis Sci 2003; 44:521-8.
54. Pugliese G, Pricci F, Romeo G, Pugliese F, Mene P, Giannini S, Cresci B, Galli G, Rotella CM, Vlassara H, Di Mario U. Upregulation of mesangial growth factor and extracellular matrix synthesis by advanced glycation end products via a receptor-mediated mechanism. Diabetes 1997; 46:1881-7.
55. DeGroot J, Verzijl N, Wenting-Van Wijk MJ, Bank RA, Lafeber FP, Bijlsma JW, TeKoppele JM. Age-related decrease in susceptibility of human articular cartilage to matrix metalloproteinase-mediated degradation: the role of advanced glycation end products. Arthritis Rheum 2001; 44:2562-71.
56. Wojcikiewicz RJ. Regulated ubiquitination of proteins in GPCR-initiated signaling pathways. Trends Pharmacol Sci 2004; 25:35-41.
57. Liu Z, Miers WR, Wei L, Barrett EJ. The ubiquitin-proteasome proteolytic pathway in heart vs skeletal muscle: effects of acute diabetes. Biochem Biophys Res Commun 2000; 276:1255-60.
58. Rodriguez T, Busquets S, Alvarez B, Carb N, Agell N, Lpez-Soriano FJ, Argils JM. Protein turnover in skeletal muscle of the diabetic rat: activation of ubiquitin-dependent proteolysis. Int J Mol Med 1998; 1:971-7.
59. Santos-Marques CI, Pereira PC. Regulation of ubiquitin proteasome pathway by methlyglyoxal in lens epithelial cells. ARVO Annual Meeting; 2004 April 25-29; Fort Lauderdale (FL).

The print version of this article was created on 27 Dec 2004. This reflects all typographical corrections and errata to the article through that date. Details of any changes may be found in the online version of the article.